Article

Primary-Frequency-Regulation Coordination Control of Wind Power Inertia and Energy Storage Based on Compound Fuzzy Logic

Suliang Ma [1], **Dixi Xin** [2,*], **Yuan Jiang** [2], **Jianlin Li** [1], **Yiwen Wu** [1] **and Guanglin Sha** [3]

[1] Electrical and Control Engineering College, North China University of Technology, Beijing 100144, China; msl13811581885@ncut.edu.cn (S.M.); ncutljl@sina.com (J.L.); wuyiwen1@mail.ncut.edu.cn (Y.W.)
[2] Automation and Electrical Engineering College, University of Science and Technology Beijing, Beijing 100083, China; jiangyuan@ustb.edu.cn
[3] Distribution Technology Center, China Electric Power Research Institute, Beijing 100192, China; guanglinsha@sina.com
[*] Correspondence: 2018311010111@mail.ncut.edu.cn

Abstract: The increasing proportion of wind power systems in the power system poses a challenge to frequency stability. This paper presents a novel fuzzy frequency controller. First, this paper models and analyzes the components of the wind storage system and the power grid and clarifies the role of each component in the frequency regulation process. Secondly, a combined fuzzy controller is designed in this paper, which realizes the cooperative control of frequency regulation considering wind power running state, battery energy management, and power grid stability. Finally, this paper establishes typical operation scenarios of various time scales to verify the effectiveness and feasibility of the proposed control strategy.

Keywords: energy storage; wind power; frequency regulation; fuzzy control; droop control coefficient

1. Introduction

New energy, such as wind power, is gradually replacing the dominance of traditional fossil energy sources. The volatility and uncertainty of wind power itself make the frequency stability of the power grid operation significantly affected [1–4]. The wind turbine does not have an active inertia response and primary frequency regulation capability. It requires additional power backup through rotor overspeed control and pitch angle control, which restricts wind power grid-connected efficiency improvement.

The wind storage system is favorable to improving the frequency stability of the system. If wind power is individually frequency-regulated, there may be transient fluctuations in frequency due to insufficient reserve power. If the storage alone is involved in frequency regulation, the required capacity configuration is too large and does not take full advantage of the wind turbine. Therefore, energy storage and wind power must be synergistically controlled during frequency regulation to utilize the performance fully.

The feasibility of wind storage systems participating in frequency regulation has been extensively studied. In reference [4], a combined wind and flywheel system is proposed, where the wind turbine always operates in MPPT mode, and the flywheel energy storage provides the inertial response and primary frequency regulation power for the system to simulate the generator. Reference [5] investigated system frequency regulation by releasing the kinetic energy of the wind turbine rotor. For large-scale wind power grid-connected power systems, wind power is required to provide primary frequency regulation, and wind turbines operating at the maximum output cannot provide power backup to meet the frequency regulation demand. References [6,7] designed a wind turbine with a variable coefficient by maintaining frequency regulation power reserve through overspeed load

shedding and paddle pitch angle control. References [8–10] studied the market mechanism and economic effect of the participation of a wind power and energy storage system in frequency regulation. It showed the feasibility of wind power and energy storage system participation in frequency regulation. References [11,12] established a battery selection system for participating in frequency regulation. References [13,14] proposed using distributed energy storage aggregation for frequency regulation to fully utilize frequency regulation resources.

The mechanism of the frequency response action of power systems is too complex and difficult to be accurate for transient states, and wind storage systems bring more uncertainty to the power system. Reference [15] proposed a frequency regulation control approach for energy storage participation using a disturbance observer, which relies on accurate modeling of the system, and then the identification of disturbance parameters after the introduction of wind power becomes a major factor limiting the application of this scheme. The study of reference [16,17] shows that the wind storage system using virtual inertia is beneficial for frequency stabilization. Reference [18] proposed an adaptive control method using a sliding film to cope with the variation in the system parameters. References [19–21] used a fuzzy control method to control the frequency regulation power of the energy storage in the wind storage system to improve its immunity to disturbances.

This paper investigates a new primary frequency regulation control method for wind energy storage systems. The method comprehensively considers wind speed, grid frequency, and SOC factors and optimizes the controller mechanism using composite fuzzy logic. The method achieves the cooperative control of wind power and energy storage during frequency regulation, improves the response speed of the wind power system to frequency perturbation, and improves the efficiency of energy storage frequency regulation utilization. In this paper, the effectiveness of the proposed strategy is verified by establishing multiple time-scale scenario models.

2. Frequency Regulation System Model of Wind Storage System

To study the effect of a wind storage system on frequency regulation characteristics, modeling the power system containing the wind storage system is the first step. The frequency regulation model uses mathematical equations to describe the frequency disturbance's influence range and propagation process. The frequency regulation model of a power system with a wind storage system includes generation, load, wind power, and battery.

2.1. Generation-Load Model

The generation-load model is used to characterize the effects of frequency disturbances in conventional power systems and the frequency regulation characteristics based on the generator swing equation. The structure of the generation load model is shown in the figure and consists of three parts: the prime mover, the generator, and the grid load.

The prime mover and generator are the core components of an electric power system to convert thermal or kinetic energy into electrical energy. In the frequency regulation process, they exhibit inertial characteristics due to their mechanical structure, which is represented in the frequency regulation model by Equation (1).

$$\begin{cases} \Delta P_\mathrm{m} = \frac{1}{(1+sT_\mathrm{R})}G_\mathrm{c}(\Delta f) \\ \Delta P_\mathrm{G} = \frac{1}{(1+sT_\mathrm{G})}\Delta P_\mathrm{m} \end{cases} \tag{1}$$

where Δf is the change in frequency, G_c is the frequency regulation control rule, T_R is the inertia coefficient of the prime mover, ΔP_m is the increment of the prime mover power, and T_G is the inertia constant of the generator. ΔP_G is the increment of generator power.

In the frequency regulation of power systems, generators mainly provide inertial action to maintain the system's stability. The inertia time constant represents the ability of the generator to provide inertia. For power systems containing new energy sources, the overall

inertia time constant decreases as the penetration of new energy sources increases [22–24]. The inertia and system inertia constant formula was calculated, as shown in Equation (2).

$$
\begin{cases}
H = \frac{P_A}{P_G} = \frac{(e^2-1)J\omega_{g,max}^2}{2e^2 P_G} \\
\eta = \frac{P_W}{P_W + P_G} \\
H_\eta = \frac{\sum P_A}{\sum P_W + \sum P_G} = (1-\eta)H
\end{cases}
\tag{2}
$$

where H is the inertia time constant; P_A is the inertia regulated power of thermal unit; P_G is the rated power of the generators; P_W is the rated power of the wind turbine; η is the new energy penetration rate; H_η is the inertia time constant under high penetration; and e is the regulation depth.

The load presents a damping effect on frequency regulation. For frequency fluctuations in a limited range, the damping effect of the load on frequency can be linearized locally. Similarly, the inertial characteristics of the generator can be treated. The generator–load model can be obtained by combining the generator's inertial action and the load's damping characteristics, as in Equation (3):

$$
\begin{cases}
\Delta P_m - \Delta P_e = 2(1-\eta)H\frac{df}{dt} \\
\Delta P_e = \Delta P_L + \Delta P_{fL} = \Delta P_L + D\Delta f \\
\Delta P_m + \Delta P_L = (2(1-\eta)H + D)\Delta f
\end{cases}
\tag{3}
$$

where ΔP_m is the variation in mechanical power; ΔP_e is the variation in electromagnetic power; ΔP is the variation in load power; ΔP_{fL} is the response power of a load for frequency; and D is the load damping.

2.2. The Wind Model

Wind turbines are mechanical, electrical, and control devices that convert wind speed into electrical energy. Wind speed at long time scales is represented using a Weibull distribution model:

$$
f_{W(s,k)} = \frac{k}{s}\left(\frac{v}{s}\right)^{k-1} \exp\left[-\left(\frac{v}{s}\right)^k\right]
\tag{4}
$$

where $f_{W(s,k)}$ is the corresponding wind speed occurrence probability, s is the scale parameters, k is the shape parameters.

Wind power is affected by the randomness of wind speed, and the wind speed variation process can be represented using a combined wind speed model consisting of basic wind speed, gust wind speed, asymptotic wind speed, and random wind speed:

$$
\begin{cases}
V_w = V_b + V_g + V_r + V_n \\
V_b = s\Gamma\left(1 + \frac{1}{K}\right) \\
V_g = \frac{V_{g,max}}{2}\left[1 - \cos\left(2\pi * \left(\frac{t - t_{g1}}{T_g}\right)\right)\right] \\
V_r = V_{r,max}\frac{t - t_{r1}}{t_{r2} - t_{r1}} \\
V_n = V_{n,max}R_{am}(-1,1)\cos(\omega_n t + \varphi_n)
\end{cases}
\tag{5}
$$

where V_w is the combined wind speed; V_b is the basic wind speed; V_g is the gust wind speed; V_r is the asymptotic wind speed; V_n is the random wind speed; Γ is the gamma function; $V_{g,max}$ is the max speed of gust wind; t_{g1} is the start time of gust wind; T_g is the duration of gust wind; $V_{r,max}$ is the max speed of asymptotic wind; t_{r1} is the start time of asymptotic wind; t_{r2} is the ending time of asymptotic wind; $V_{n,max}$ is the max speed of random wind; R_{am} is a uniform random number with values between -1 and 1; ω_n is the rate of change in fluctuation; and φ_n is a uniform random number with values between 0 and 2π.

The wind power model is used to represent the output of a wind turbine based on wind power and changes in the state of the power system. The wind turbine output power is shown in Equation (6).

$$\begin{cases} P_w = \frac{1}{2}\pi\rho R^2 v_w^3 C_p(\lambda, \beta) \\ \lambda = \frac{\omega_r R}{v_w} \end{cases}$$ (6)

where ρ is the air density, R is the wind turbine blade radius, λ is the blade tip speed ratio, β is the pitch angle, ω_r is the wind turbine rotor speed, and C_p is the wind power utilization factor of wind turbines.

$$\begin{cases} C_p = 0.5176(\frac{116}{\lambda_i} - 0.4\beta - 5)e^{-\frac{21}{\lambda_i}} + 0.0068\lambda \\ \frac{1}{\lambda_i} = \frac{1}{\lambda + 0.08\beta} - \frac{0.035}{\beta^3 + 1} \end{cases}$$ (7)

When the wind speed is between the cut-in wind speed and the rated wind speed, and the pitch angle is set to zero, there exists the optimal blade tip speed ratio λ_{opt}. At this time, the wind turbine is at the optimal operating point and has the maximum wind power utilization coefficient $C_{p,max}$.

$$\begin{cases} \frac{\partial C_p}{\partial \lambda}\Big|_{\beta=0, \lambda=\lambda_{opt}} = 0 \\ C_{p,max} = C_p(\lambda_{opt}, 0) \end{cases}$$ (8)

In a wind power generation system with a high percentage, when the wind turbines are required to provide frequency support capability, the wind turbines need to operate at a reduced load under the maximum power point to provide standby power, and the power provided by the wind turbines under reduced load operation is expressed as follows:

$$\begin{cases} P_{w,d} = (1-d)P_w = 0.5\pi\rho R^2 v_w^3(1-d)C_{p,max} \\ C_{p,d} = (1-d)C_{p,max} \\ P_{w,del} = P_w - P_{w,d} = dP_w \end{cases}$$ (9)

where $P_{w,d}$ is the output power of the wind turbine under load shedding control, $P_{w,del}$ is the power lost under load shedding control, and d is the load shedding factor.

Due to the mechanical structure's influence, the wind turbine's dynamic process involved in frequency regulation shows inertial characteristics [25–27]. The control strategy for wind power using load-shedding power as backup power and using virtual inertia control for frequency regulation is shown in Figure 1.
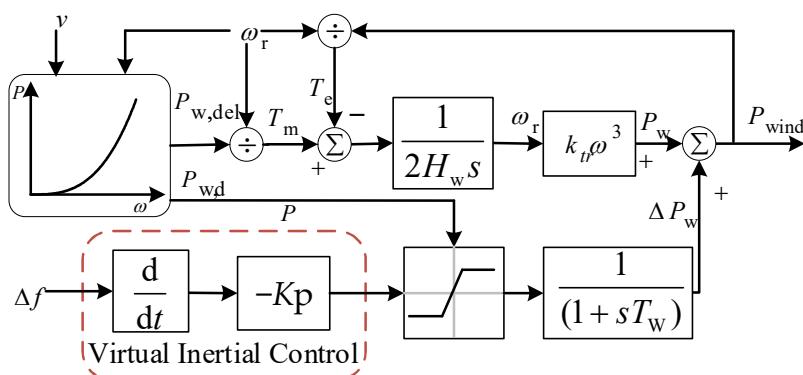

Figure 1. Control block diagram of wind turbine.

In this figure, T_m and T_e are the mechanical torque and electromagnetic torque, respectively. H_w is the inertia time constant of the wind turbine. k_t is the power tracking factor. T_w is the response time factor of wind power regulation. k_p is the inertial control coefficient.

2.3. The Battery Model

Batteries are suitable as a complement to frequency regulation resources due to their faster response and energy storage characteristics. A battery-based energy storage system consists of a battery body, an energy storage converter, and an energy management system. The battery can be considered a flow-controlled voltage source with a capacity limit. The equivalent circuit simulates the external characteristics of the battery using devices such as resistors, capacitors, and constant voltage sources. The equivalent model has multiple topological structures, and the basic form of the model is as follows:

$$\begin{cases} SOC(t + \Delta t) = SOC(t) + \frac{I_b \times \Delta t}{Q_{max}} \\ I_b = \frac{P_B}{V_{ocv} - U_d(R,C,I_b)} \\ P_{B,min} \le P_B \le P_{B,max} \\ SOC_{min} \le SOC \le SOC_{max} \end{cases} \tag{10}$$

where Q_{max} is the maximum discharge capacity of the battery; Δt is the sampling time interval; I_b is the charging/discharging current of the battery and V_{ocv} is the open circuit voltage; U_d is the voltage droop during battery operation, which is a function of the internal resistance and capacitance parameters of the battery; and $P_{B,min}$, $P_{B,max}$, SOC_{min}, and SOC_{max} are the minimum output power, maximum output power, and minimum and maximum SOC values of the supercapacitor, respectively.

In frequency regulation, the power response rate of the battery is mainly influenced by the controller and the energy storage converter. This process can be simplified without loss of generality to an inertial process, as shown below:

$$\Delta P_B = \frac{1}{(1 + sT_B)} \Delta P_{B,ref} \tag{11}$$

where T_B is the regulation response time factor of energy storage.

From the above analysis, it is clear that the battery has good frequency regulation performance. The battery's service life is the main influencing factor that restricts energy storage participation in frequency regulation. Relevant studies have shown that the charging/discharging rate and the charging and discharging depth affect the battery's service life [28,29]. Using excessive current charging/discharging in the frequency regulation process will directly cause the loss of battery life. In addition, excessive energy storage participation in frequency regulation will cause a deepening of the discharge depth, further affecting the battery's service life. The conventional approach is to design an energy allocation strategy based on a logistic function, as shown in Equation (12):

$$\begin{cases} k_{ch} = \frac{P_0 \times e^{0.5n \times (SOC_{max} - SOC)}}{K_{max} + P_0 \times \left(e^{0.5n \times (SOC_{max} - SOC)} - 1\right)} \\ k_{dis} = \frac{P_0 \times e^{0.5n \times (SOC - SOC_{min})}}{K_{max} + P_0 \times \left(e^{0.5n \times (SOC - SOC_{min})} - 1\right)} \end{cases} \tag{12}$$

where k_{ch} and k_{dis} is the charging and discharging factor, n is the adaptive factor to measure the degree of fast or slow curve change; P_0 is the initial power; K_{max} is the factor maximum; and SOC is the SOC value at the current moment.

3. Compound Fuzzy Logic Primary-Frequency-Regulation Cooperative Control Strategy

3.1. Frequency Control Model

After a disturbance occurs in the power system, its active frequency dynamic process is divided into three stages: automatic distribution of disturbance power according to the synchronous power coefficient, inertial response, and frequency regulation. In the disturbance-power allocation stage, each generator shares the disturbance power instantaneously according to its synchronous power coefficient with the disturbance point. In the inertia response stage, after the power deficit occurs, the electromagnetic power changes

abruptly, the mechanical power remains unchanged, the rotor changes under the action of unbalanced torque according to the rotor equation of motion, and the speed droops to release kinetic energy and resist the system frequency droop. When the system frequency exceeds the governor threshold, the governor system is a frequency regulation action to restore the system frequency to the allowable range, followed by secondary and tertiary frequency regulation successive actions to restore the system frequency and achieve the economic power distribution between the units. The model of the frequency regulation system studied in this paper is shown in Figure 2.
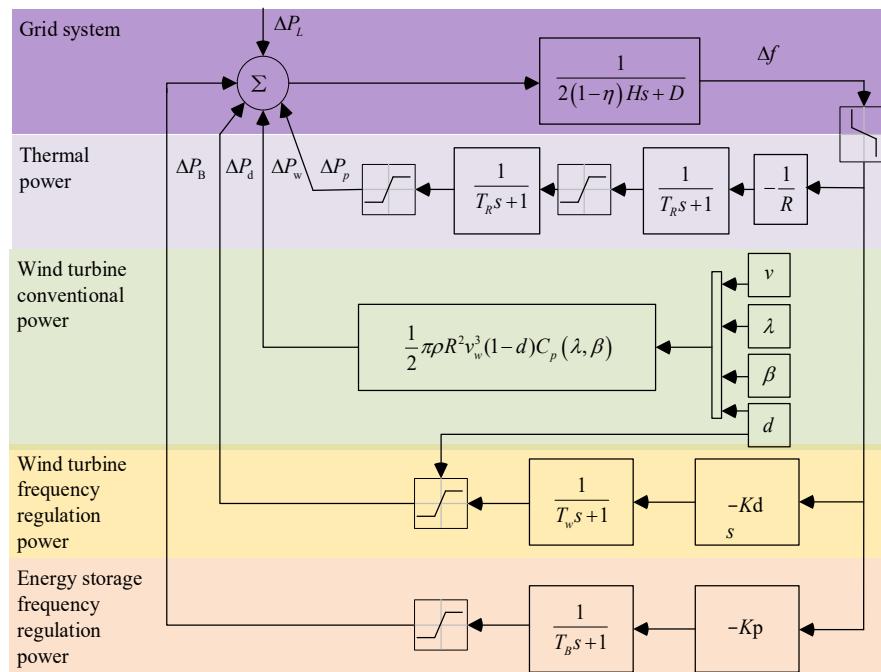

Figure 2. Control block diagram of the studied frequency regulation.

The generator system, wind power system, and energy storage system in the grid assume different roles in the frequency regulation process due to their respective characteristics: the generator system is used to provide rotational inertia; the wind power system is used as a supplement to the generator supply to provide current-source virtual inertia; and the energy storage system is used as a regulator to provide voltage-source virtual inertia. The frequency regulation process needs to satisfy the following energy balance relationship:

$$\Delta P_{\mathrm{L}} + \Delta P_{\mathrm{w}} = \Delta P_{\mathrm{p}} + \Delta P_{\mathrm{d}} + \Delta P_{\mathrm{B}} \tag{13}$$

where ΔP_{L} is the power disturbance from the load; ΔP_{w} is the disturbance from the wind power; ΔP_{p} is the primary frequency regulation power of the thermal power unit; ΔP_{d} is the virtual inertia power based on wind power; and ΔP_{B} is the frequency regulation power provided by the battery.

The generator system mainly provides rotational inertia during primary frequency regulation. A droop factor controls the generator set during primary frequency regulation:

$$\Delta P_{\mathrm{p}} = -\frac{1}{R} \Delta f \tag{14}$$

where R is the adjustment coefficient.

Wind turbines provide current-source-type virtual inertia in the frequency regulation process. Current-source virtual inertia control is to introduce the system frequency change rate into the converter active control link, change the active reference value, and provide

active power to the grid proportional to the frequency change rate; the equation for this is as follows:

$$\Delta P_{\text{d}} = -\text{Kd}\frac{\text{d}\Delta f}{\text{d}t} \tag{15}$$

where Kd is the virtual inertia control coefficient.

The energy storage system complements the frequency regulation and presents a voltage-source-type virtual inertia characteristic. The voltage-sourced virtual inertia technique introduces additional control variables in the converter control to invoke energy storage or standby power to give it the external characteristics of a synchronous unit operating in grid-connected mode. Due to the inertia limitation of the energy storage converter and the body response, the external characteristics of the energy storage involved in frequency regulation show sagging characteristics. In addition, the battery needs to consider the effect of its characteristics, such as SOC. The control of the battery follows Equation (16):

$$\Delta P_{\text{B}} = -m\text{Kp}\Delta f \tag{16}$$

where Kp is the droop control coefficient; m is the charge/discharge control factor.

3.2. Fuzzy Control Model

The control coefficients of different power resources need to be set during frequency regulation. Fixed parameters are usually used for frequency regulation control for generating units in conventional power systems and a high percentage of new energy systems.

For the frequency regulation of a high percentage of new energy power systems, the control coefficients of wind power and energy storage need to be adjusted according to the energy balance state of the grid, the wind speed condition, and the battery state. When the set control parameters are less than the system demand, the power output of the frequency regulation resources in the system cannot meet the system demand, which will cause the fluctuation of the frequency index to cross the limit; when the control setting parameters are greater than the system demand, the frequency regulation resources in the system are frequently called to cause the system to lose stability.

However, it is difficult to establish an accurate mathematical model between the value of control coefficients and wind conditions, the rate of change in frequency difference, and frequency deviation. Fuzzy logic-based control has the advantages of ease, high robustness, and high fault tolerance. Among them, the inertia control coefficient of wind power and the droop control coefficient of the battery are influenced by wind speed, frequency, and frequency variation rate; the charging and discharging coefficients of the battery are influenced by the operating state and state of charge (SOC).

In Figure 3, I_{ch} and I_{dis} are the charging and discharging current.
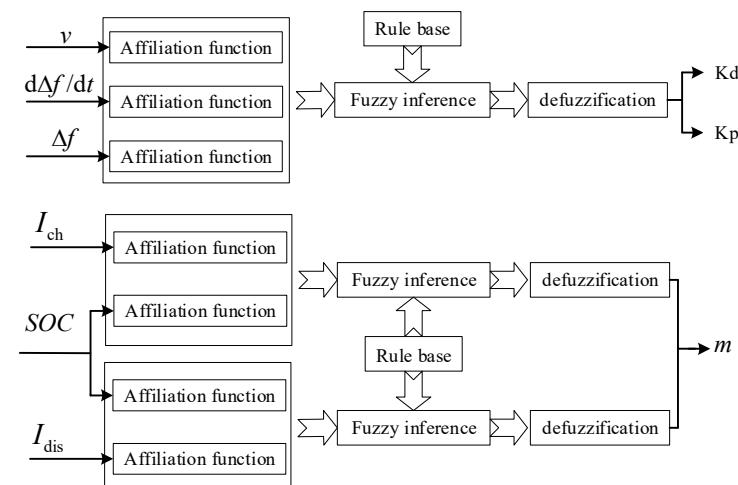
Figure 3. Control block diagram of the proposed fuzzy control strategy.

The theoretical domain of the wind speed is taken as [6, 13.5] m/s, the theoretical domain of the frequency difference rate of change is taken as [−0.6, 0] Hz/s, the theoretical domain of the frequency deviation amount is taken as [−1, −0.033] Hz, and the theoretical domain of both the virtual inertia coefficient and the sag coefficient is taken as [5, 20]. These are fuzzy language variables with {VS, S, M, B, VB} values. The affiliation function is shown in Figures 4 and 5.
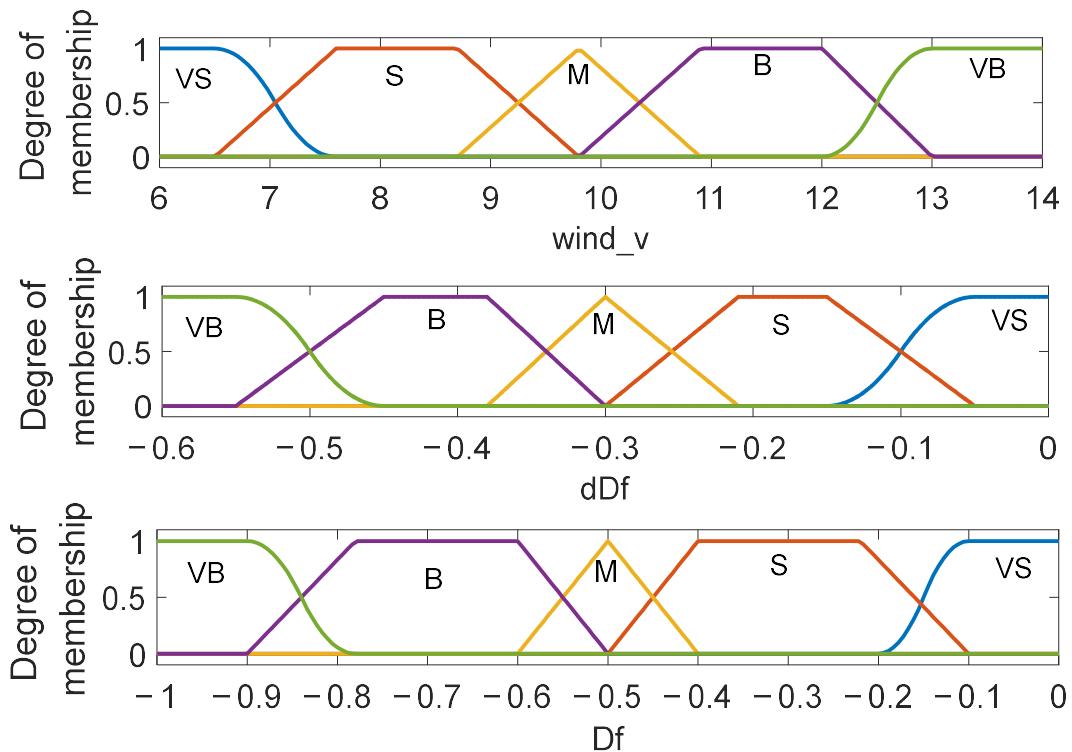

Figure 4. The membership function of input variable in the proposed fuzzy control strategy.
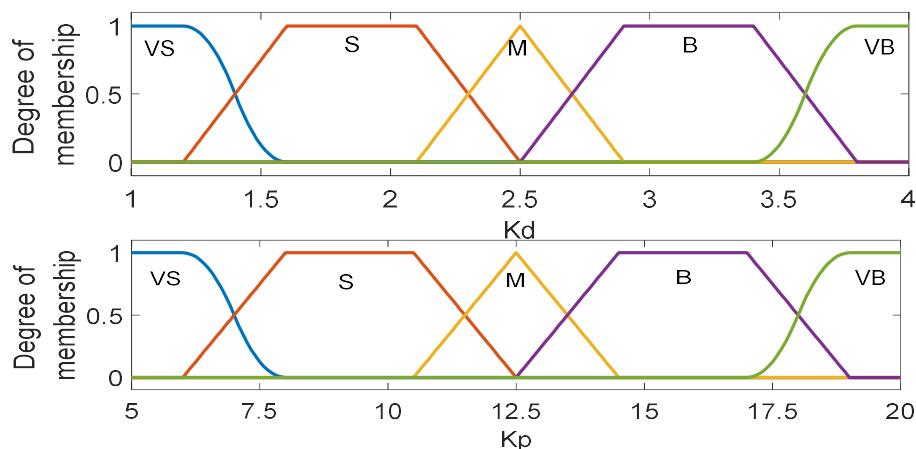
Figure 5. The membership function of the output variable in the proposed fuzzy control strategy.

The Kd and Kp correspond to the degree of involvement of wind power and energy storage in frequency regulation, respectively. Kd represents the degree of frequency regulation participation of wind power. When the wind power resources are more sufficient, the value of Kd should be adjusted to achieve the purpose of fully utilizing the resources; Kp represents the degree of participation in the frequency regulation of energy storage when there is a large frequency disturbance in the power system; and Kp should be adjusted up

to achieve the purpose of making full use of the fast response of energy storage. The design of fuzzy logic rules follows the following principles, which is depicted in Table 1.

(1) When the wind speed is low, the frequency regulation ability of wind power generation is relatively weak, and too much change in rotor speed easily triggers the wind turbine off-grid. Therefore, the virtual inertia coefficient Kd should be set to a small value regardless of the change in frequency difference and frequency deviation, and it decreases with the increase in the frequency change rate; meanwhile, the energy storage should undertake the main task of frequency regulation, and Kp increases with the increase in the frequency change rate. With the increasing frequency deviation, Kd and Kp should also be increased appropriately.

(2) When the wind speed is moderate, wind power has the strongest frequency regulation ability. To maximize the wind power regulation, Kd is set with the increase in the rate of change in the frequency and decreases, Kp is set with the increase in the rate of change in frequency and increases, and Kd, Kp are set with the increase in frequency deviation and increase. When the frequency variation rate and frequency deviation are small, to avoid the battery being dispatched frequently, the value of Kd can be increased appropriately, and the value of Kp should be small; when the frequency variation rate is low, and the frequency deviation is large, the values of Kd and Kp should be large; when the frequency variation rate is large, and the frequency deviation is small, the values of Kd and Kp should be small; when the frequency variation rate and frequency deviation are large, the value of Kd should be small, and the value of Kp should be large. The Kp value should be taken as large as possible.

(3) When the wind speed is large, the regulating ability of the wind turbine is weak, and the output frequency regulation active capacity is small. When the frequency change rate is small, the value of Kd can be increased appropriately, and Kd decreases with the increase in the frequency change rate. However, when the wind speed is too large, Kd should not take too large a value, while the value of Kp is positively correlated with the frequency deviation and frequency change rate; when the frequency change rate is large, to avoid excessive release of kinetic energy, Kd should be small, and Kp can be increased appropriately. The corresponding fuzzy rule table is shown below.
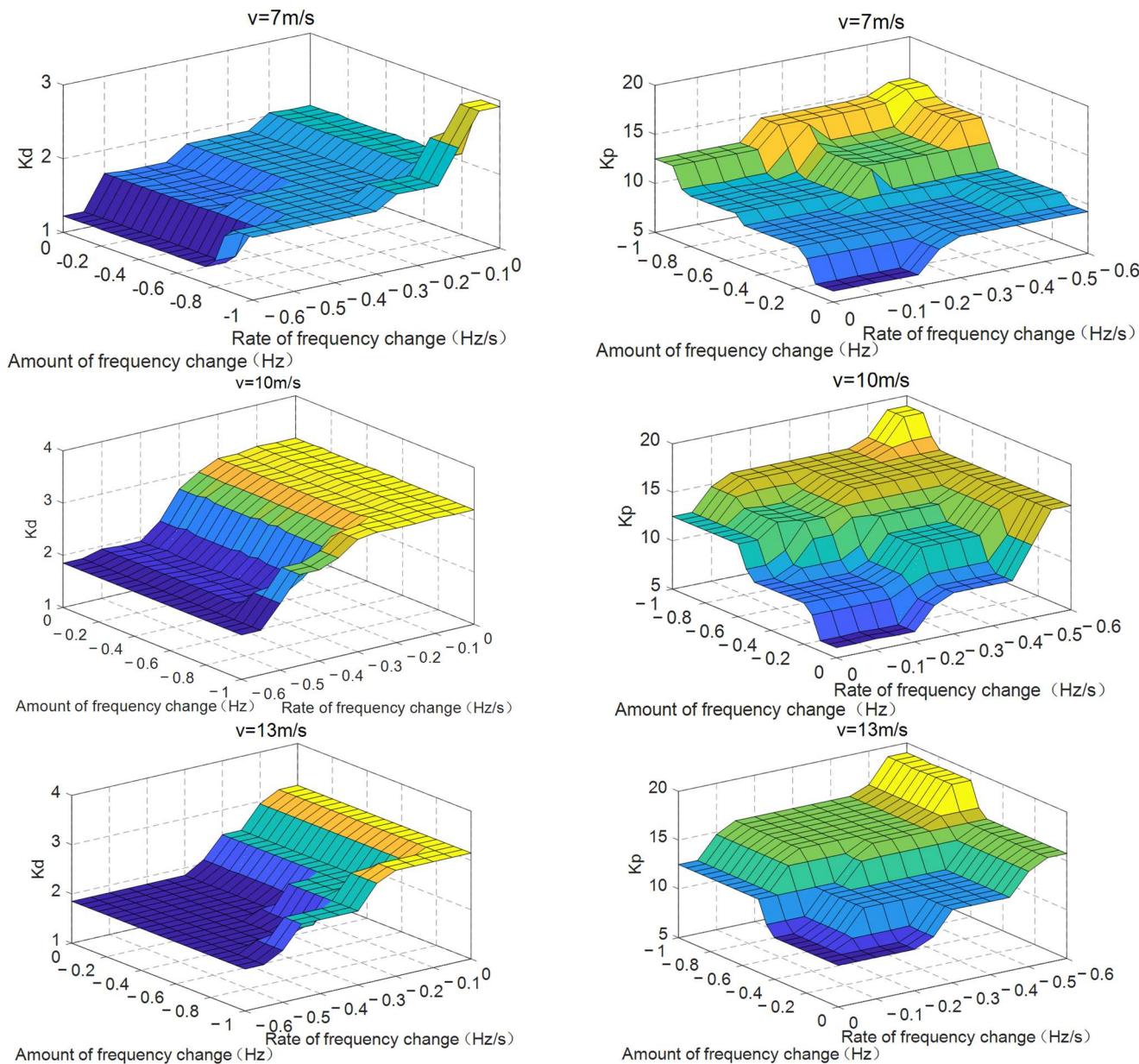
Table 1. The fuzzy control rules of control factor (Kd, Kp).

$(\frac{\mathrm{d}\Delta f}{\mathrm{d}t}, \Delta f)$	v				
	VS	**S**	**M**	**B**	**VB**
(VS, VS)	(S, VS)	(M, VS)	(B, VS)	(VB, VS)	(B, S)
(VS, S)	(S, S)	(M, S)	(B, S)	(VB, S)	(B, S)
(VS, M)	(S, S)	(M, S)	(B, S)	(VB, S)	(B, M)
(VS, B)	(S, S)	(M, M)	(B, M)	(VB, M)	(B, M)
(VS, VB)	(M, M)	(B, M)	(B, M)	(VB, M)	(B, M)
(S, VS)	(S, VS)	(S, VS)	(B, VS)	(B, VS)	(M, S)
(S, S)	(S, S)	(S, S)	(B, S)	(B, S)	(M, M)
(S, M)	(S, S)	(S, S)	(B, M)	(B, M)	(M, M)
(S, B)	(S, S)	(S, M)	(B, M)	(B, B)	(M, B)
(S, VB)	(S, M)	(M, M)	(B, B)	(VB, B)	(B, B)
(M, VS)	(S, S)	(S, S)	(M, S)	(B, S)	(S, M)
(M, S)	(S, S)	(S, S)	(M, M)	(B, M)	(S, M)
(M, M)	(S, M)	(S, M)	(M, M)	(B, B)	(S, B)
(M, B)	(S, M)	(S, M)	(M, B)	(B, B)	(M, B)
(M, VB)	(S, M)	(S, B)	(B, B)	(B, B)	(M, B)
(B, VS)	(VS, S)	(S, S)	(S, S)	(VB, M)	(S, M)
(B, S)	(VS, S)	(S, S)	(S, M)	(B, B)	(S, M)
(B, M)	(VS, S)	(S, M)	(S, M)	(B, B)	(S, B)
(B, B)	(S, S)	(S, B)	(S, B)	(M, B)	(S, B)
(B, VB)	(S, M)	(S, B)	(M, B)	(B, B)	(M, B)

Table 1. *Cont.*

$(\frac{\mathrm{d}\Delta f}{\mathrm{d}t}, \Delta f)$	v				
	VS	**S**	**M**	**B**	**VB**
(VB, VS)	(VS, S)	(VS, S)	(S, B)	(S, B)	(S, B)
(VB, S)	(VS, S)	(VS, M)	(S, B)	(S, B)	(S, B)
(VB, M)	(VS, M)	(VS, M)	(S, B)	(S, B)	(S, B)
(VB, B)	(S, M)	(VS, B)	(S, B)	(S, B)	(S, VB)
(VB, VB)	(S, B)	(S, B)	(S, VB)	(S, VB)	(S, VB)

The fuzzy variable relationships at different wind speeds are plotted as shown in Figure 6.

Figure 6. The fuzzy variable relationships at different wind speeds.

The output domain of the battery's charge/discharge factor controller is set to [0, 1]. The charge state domain is set to [0.1, 0.9]. The operating state of the battery is represented by the charge/discharge multiplier, which is set to [0, 1], and the following formula calculates the charge/discharge multiplier:

$$\text{rate-C} = \frac{I_{\text{ch/dis}}}{I_{\text{e}}} \tag{17}$$

where I_{e} is the rated current, and rate-Ca is the charge/discharge multiplier. The affiliation function is shown in Figure 7.
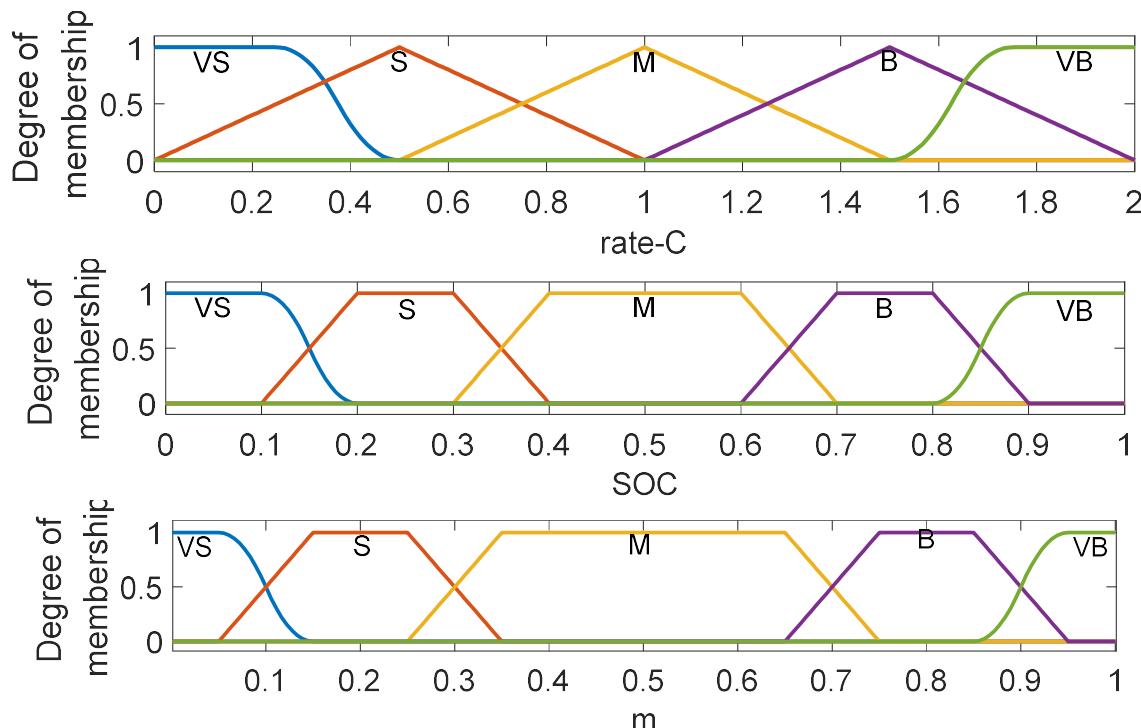
Figure 7. The membership function of the battery state.

m is used to regulate the magnitude of the energy storage output. When the charging and discharging multiplicity of the battery is too large or the SOC is too low, m should moderately reduce the limiting current to avoid over-discharge. The design of fuzzy logic rules follows the following principles, which is depicted in Tables 2 and 3.

(1) When the battery is in a discharged state, the battery needs to avoid excessive discharge at low soc. As the SOC of the battery decreases, the discharge control factor gradually decreases. To avoid insufficient power resources provided by frequency regulation, the discharge control coefficient increases with the increase in the discharge multiplier.

(2) When the battery is charging, the battery needs to avoid over-electricity in the case of high soc, and the discharge control coefficient gradually decreases as the soc of the battery increases. To avoid insufficient power resources provided by frequency regulation, the charging control coefficient increases with the increase in the discharge multiplier.

The design of fuzzy logic rules follows the following principles:
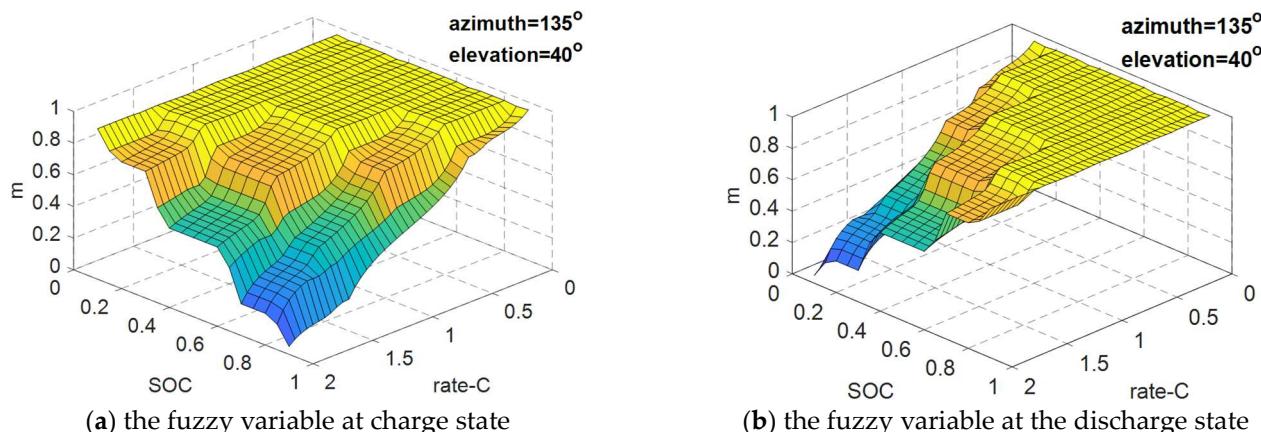
Table 2. The fuzzy logic rules at charge state.

Rate-C	SOC				
	VS	**S**	**M**	**B**	**VB**
VS	VB	VB	VB	VB	VB
S	B	VB	VB	VB	VB
M	M	B	VB	VB	VB
B	S	M	B	VB	VB
VB	VS	S	M	B	VB

Table 3. The fuzzy logic rules at discharge state.

Rate-C	SOC				
	VS	**S**	**M**	**B**	**VB**
VS	VB	VB	VB	VB	VB
S	VB	VB	VB	VB	B
M	VB	VB	VB	B	M
B	VB	VB	B	M	S
VB	VB	B	M	S	VS

The fuzzy variable relationships at the charge state and discharge state are shown as shown in Figure 8.

(**a**) the fuzzy variable at charge state   (**b**) the fuzzy variable at the discharge state

Figure 8. The fuzzy variable at charge and discharge state.

4. Case Studies and Simulations

To verify the feasibility and effectiveness of the proposed combined wind storage system to participate in the primary frequency regulation strategy, a simulation model was built on the MATLAB/Simulink platform (Matlab 2020a), as shown in the Appendix A. The proposed model had a benchmark of 160 MW, including 100 MW of thermal power units, 50 MW of wind power, and 10 MW of energy storage units. The benchmark frequency was 50 Hz, and the upper and lower dead limits of frequency regulation were set to 0.033 Hz. An energy storage configuration of 10 Mw/5 Mwh is specified in the Table 4.

Table 4. The parameters of the case.

Parameters	Value
Rated power of thermal power	100 MW
Inertia time constant of thermal power	5.8 s
Regulation response time factor of prime mover	0.25 s
Regulation response time factor of generator	0.35 s

Table 4. *Cont.*

Parameters	Value
Adjustment factor of thermal power	0.1
Rated power of wind power	50 MW
Inertia time constant of wind turbine	3 s
Regulation response time factor of wind turbine	0.3 s
Rated power of energy storage	10 MW
Rated capacity of energy storage	5 MWh
Regulation response time factor of energy storage	0.01 s
Load damping	1.2 s

4.1. Step Dynamic Performance Simulation

Power systems are typically time-varying nonlinear systems, and frequency regulators must have strong tracking performance. This study used a step response to verify the tracking rejection capability of the proposed control method for frequency disturbance rejection. The disturbance used was a 10% increase in rated power at 1 s and a 15% decrease in rated power at 15 s. We used 6 m/s as a typical low wind speed and 9 m/s as a typical high wind speed; we set the low SOC to 20%, medium SOC to 50%, and high SOC to 80%. The results at low wind speeds are shown in Figures 9–11. The results include the frequency variation, thermal-power frequency regulation power, wind-power frequency regulation power, energy-storage frequency regulation power, and parameter variation. The results were compared, including fixed parameter control and conventional fuzzy control results.
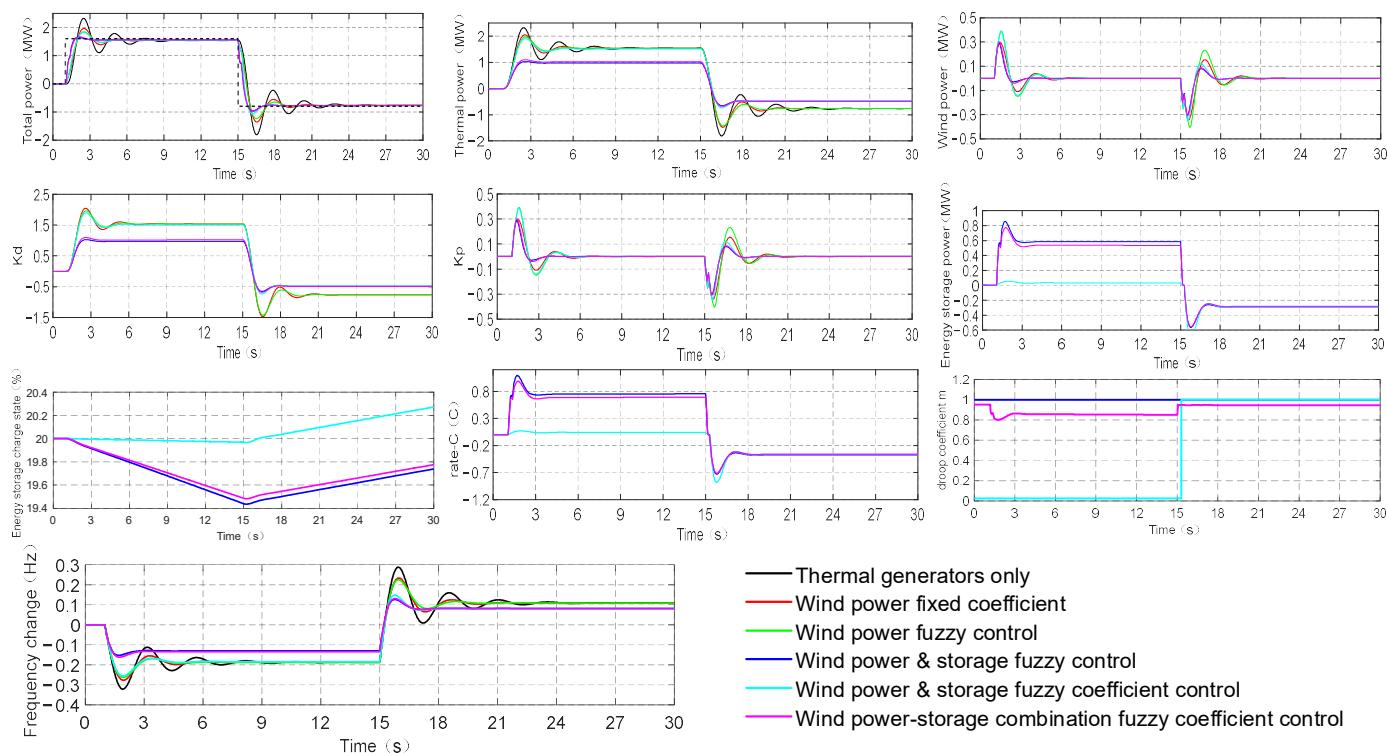
Figure 9. Simulation results at a low wind speed and low state of charge.
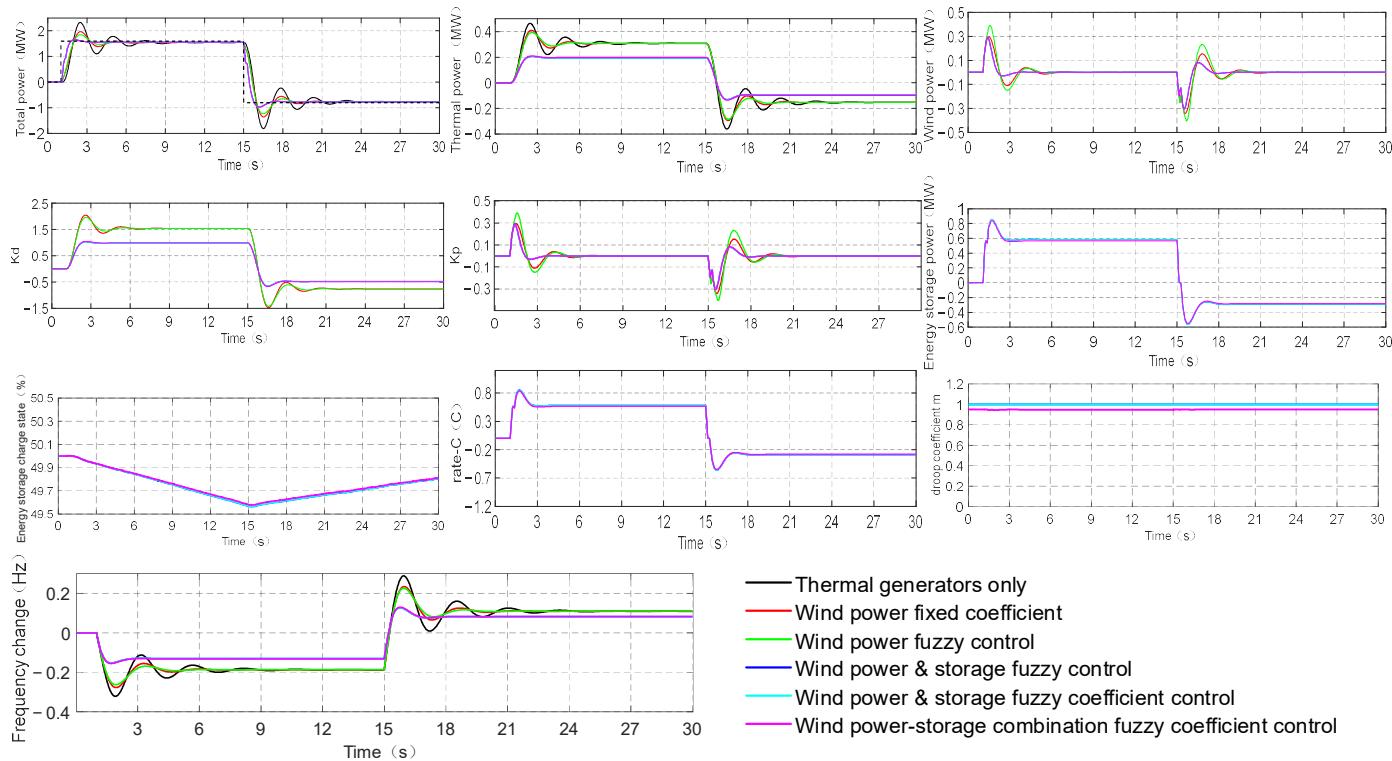
Figure 10. Simulation results at a low wind speed and medium state of charge.
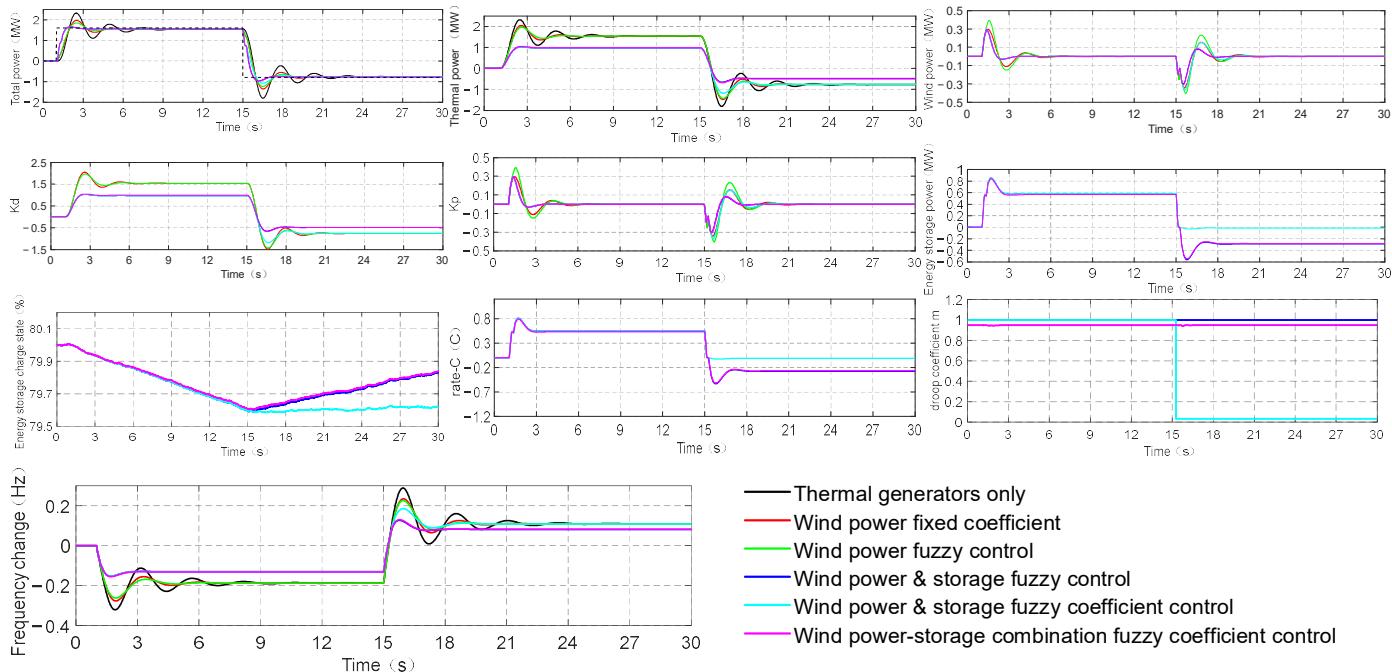
Figure 11. Simulation results at a low wind speed and high state of charge.

The working conditions used for the simulation are described below.

Case 1: Thermal generators only. Thermal power units are involved in frequency regulation, while wind power units and energy storage are not involved in frequency regulation.

Case 2: Wind-power fixed coefficient. Thermal turbines are involved in frequency regulation, energy storage is not involved in frequency regulation, and wind turbines are involved in frequency regulation using inertia control with fixed parameters; Kd is set to a constant value of −1.

Case 3: Wind power fuzzy control. Thermal units are involved in frequency regulation, energy storage is not involved in frequency regulation, and wind turbines are involved in frequency regulation using fuzzy control.

Case 4: Wind power and storage fuzzy control. Thermal units are involved in frequency regulation storage, wind turbines are involved in frequency regulation using their own independent fuzzy control, and storage is not controlled for the charging/discharging current.

Case 5: Wind power and storage fuzzy coefficient control. Thermal units are involved in frequency regulation energy storage, wind turbines are involved in frequency regulation using independent fuzzy controls, and energy storage is controlled using conventional methods for charging/discharging currents.

Case 6: Wind power–storage combination fuzzy coefficient control. Thermal units are involved in frequency regulation, while energy storage and wind turbines use the control method proposed in this paper.

The simulation results at high wind speeds are shown in Figures 12–14. The simulation results also show the ability of the proposed control strategy to suppress the frequency disturbance and adapt to the energy storage and charging state. In addition, the proposed control strategy can further improve the frequency regulation performance through dynamic regulation because the wind turbine can provide more backup power at a high wind speed.
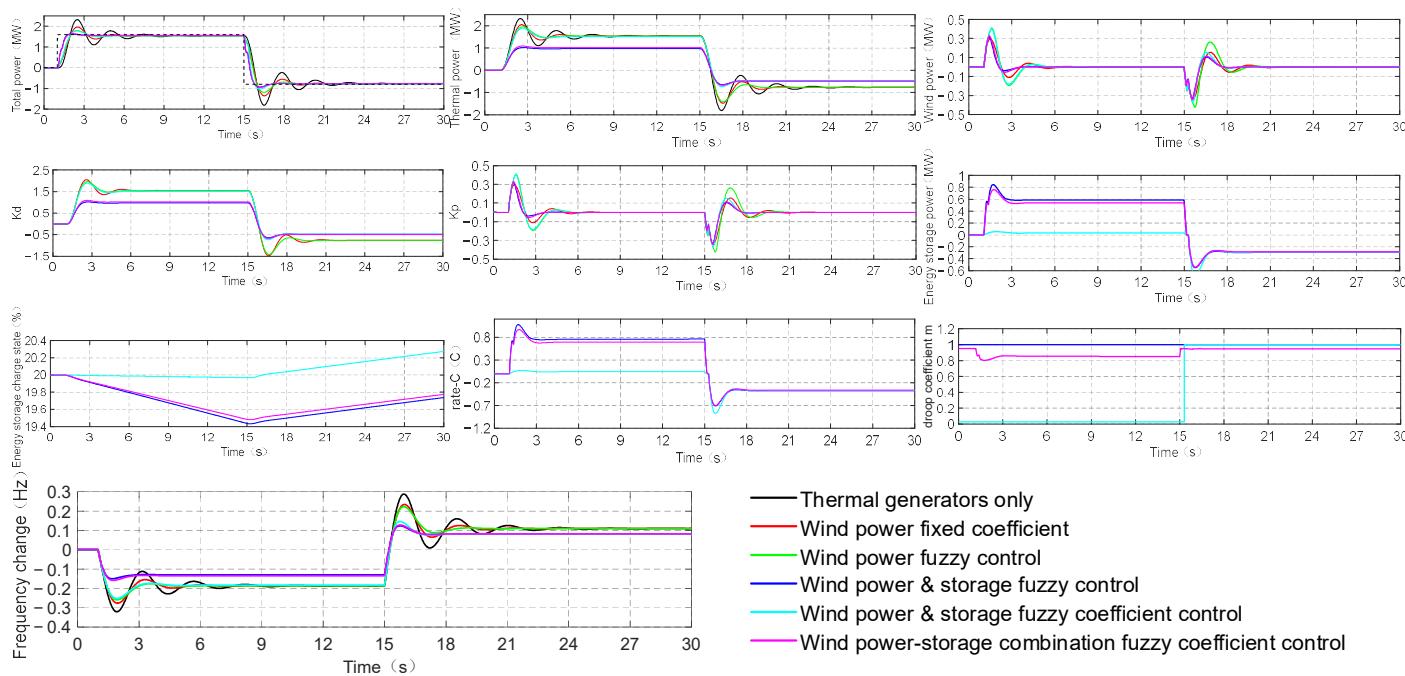
Figure 12. Simulation results at a high wind speed and low state of charge.

Tables 5 and 6 show the comparison of the resultant data at low and high wind speeds, respectively. According to the data analysis, the proposed control strategy has a significant effect on reducing the frequency variation. At a medium SOC and low wind speed, the frequency changes in Case 1 and the proposed control strategy Case 6 were 0.3212 Hz and 0.1552 Hz, respectively, and the frequency change was reduced by 0.166 Hz. At a medium SOC and high wind speed, the frequency changes in Case 1 and the proposed control strategy Case 6 were 0.3212 Hz and 0.1525 Hz, respectively, and the frequency change was reduced by 0.1687 Hz. Compared with only wind power involved in frequency regulation Case 2 and Case 3, the proposed control strategy had a significant frequency change suppression effect. At low wind speeds, the frequency variations were reduced by 0.1216 Hz and 0.1073 Hz, respectively; at high wind speeds, the frequency variations were

reduced by 0.1243 Hz and 0.11 Hz, respectively; The frequency change in the proposed control was basically the same as compared to Case 4 and 5 but there is an advantage of the proposed control strategy in terms of energy management. The proposed control strategy reduces the SOC change at any operating condition, compared to Case 4. However, Case 5 achieves charging at a low SOC change but increases the frequency change. Overall, the proposed control strategy achieves synergistic control of the frequency variation and SOC change.
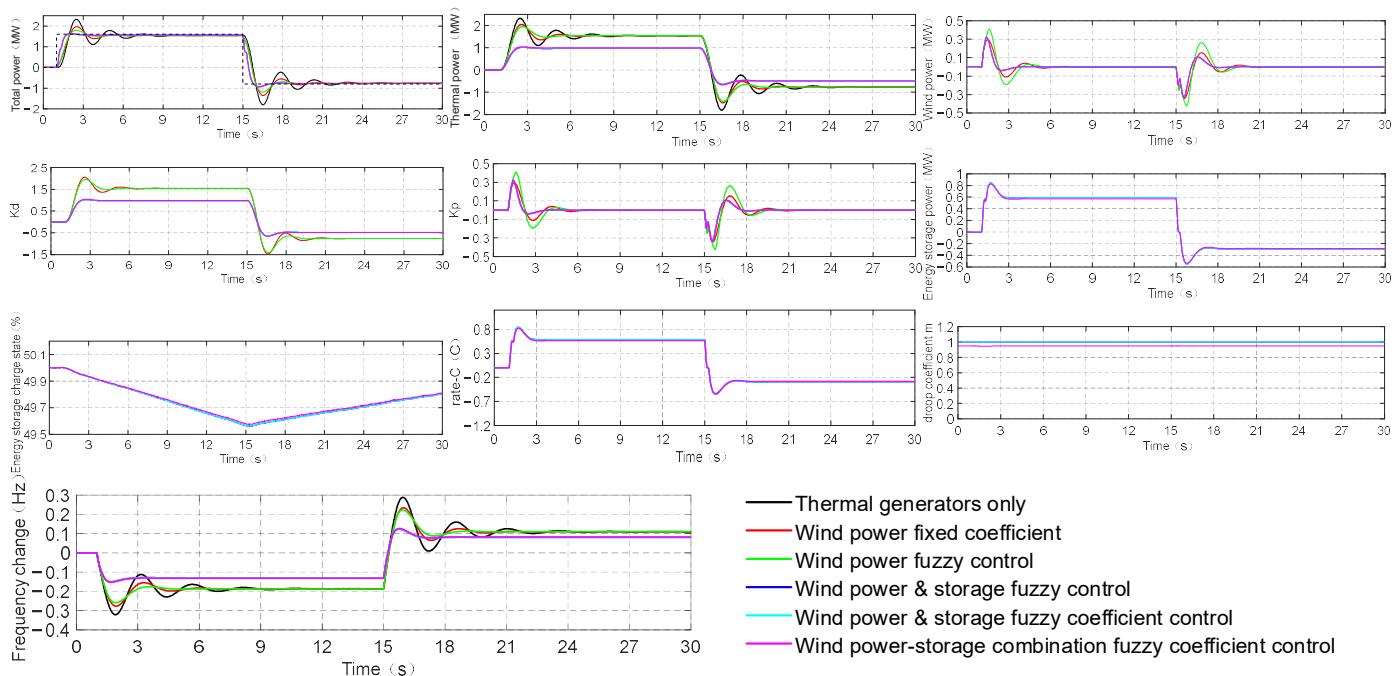
Figure 13. Simulation results at a high wind speed and medium state of charge.
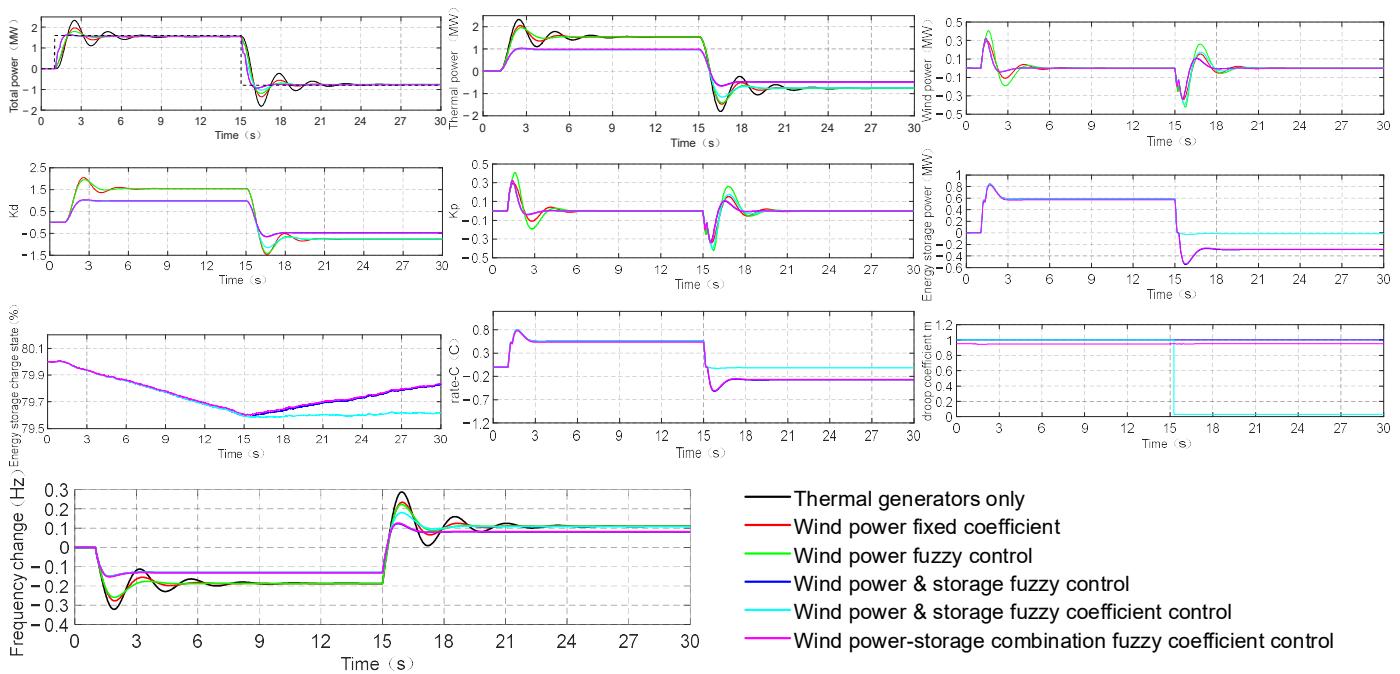
Figure 14. Simulation results at a high wind speed and high state of charge.

Table 5. Comparison of results at low wind speeds.

Parameters	Frequency Change (Hz)			SOC Change (%)		
	Low SOC	Medium SOC	High SOC	Low SOC	Medium SOC	High SOC
Case1: Thermal generators only		0.3212		/	/	/
Case2: Wind power fixed coefficient		0.2768		/	/	/
Case3: Wind power fuzzy control		0.2625		/	/	/
Case4: Wind power and storage fuzzy control	0.1528	0.1528	0.1528	−0.269	−0.1942	−0.1675
Case5: Wind power and storage fuzzy coefficient control	0.2555	0.1528	0.1528	0.2725	−0.1941	−0.3781
Case6: Wind power–storage combination fuzzy coefficient control	0.1616	0.1552	0.1552	−0.2243	−0.1876	−0.1615

Table 6. Comparison of results at high wind speed.

Parameters	Frequency Change (Hz)			SOC Change (%)		
	Low SOC	Medium SOC	High SOC	Low SOC	Medium SOC	High SOC
Case1: Thermal generators only		0.3212		/	/	/
Case2: Wind power fixed coefficient		0.2768		/	/	/
Case3: Wind power fuzzy control		0.2593		/	/	/
Case4: Wind power and storage fuzzy control	0.1501	0.1501	0.1501	−0.2624	−0.1953	−0.1686
Case5: Wind power and storage fuzzy coefficient control	0.2522	0.1501	0.1501	0.2751	−0.1953	−0.3810
Case6: Wind power–storage combination fuzzy coefficient control	0.1587	0.1525	0.1525	−0.2253	−0.1888	−0.1625

4.2. Sudden Change in Wind Speed Simulation
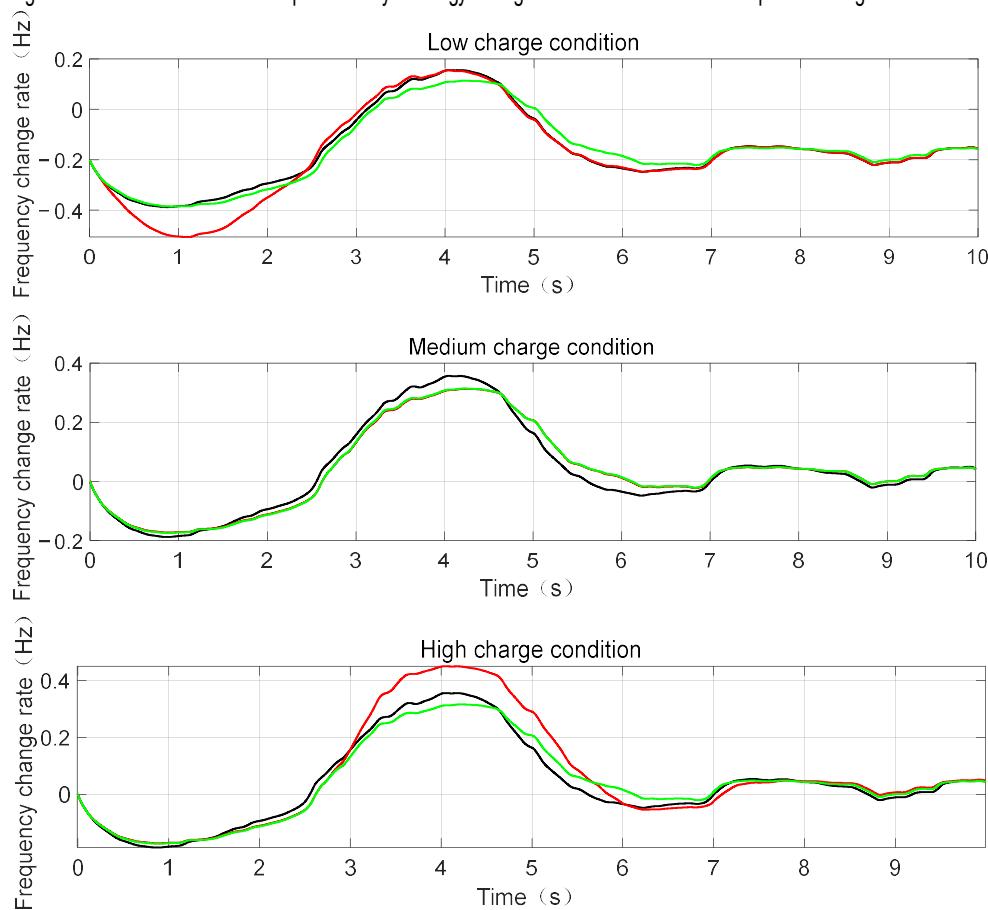
Wind speed variations affect the frequency stability characteristics of a high percentage of new energy power systems. In this paper, a combined wind speed model was used to simulate the response of the proposed control strategy to sudden wind speed changes. The basic wind speed was set to 6.2 m/s, the max speed of gust wind was set to 10 m/s, the max speed of asymptotic wind was set to 3 m/s, and the max speed of random wind was set to 1 m/s. The start time of gust wind was set to 1 s, the duration of gust wind was set to 5 s, the start time of asymptotic wind was set to 2 s, and the ending time of asymptotic wind was set to 5 s. A schematic of the wind speeds used for the simulation is shown in the Appendix A. The simulation results are shown in Figures 15–19 and Table 7.

The analysis of the simulation results shows that the proposed control strategy has a good ability to suppress the frequency disturbances caused by sudden wind speed. Compared with the wind-power-and-storage fixed coefficient, the peak value of the proposed control strategy was reduced by up to 12.2%; compared with the wind power fuzzy + energy storage control curve, the peak value of the proposed control strategy was reduced by up to 30.6%. The proposed control strategy's performance was comparable to the energy storage using the control curve under the medium storage charge state. However, in the high- or low-charge state, the energy storage regulation coefficient needs to be adjusted stepwise according to the charge/discharge state, which makes the system need more regulation time and generates additional overshoot. The proposed control strategy can achieve continuous dynamic adjustment of the energy storage control coefficient, avoiding the control of the additional introduction of disturbances and significantly improving control performance.

Table 7. Comparison of results at a sudden change in wind speed.

Parameters	Frequency Change Pack (Hz)			Final SOC (%)		
	Low Charge Condition	Medium Charge Condition	High Charge Condition	Low Charge Condition	Medium Charge Condition	High Charge Condition
Wind power and storage fixed coefficient	0.3563	0.3563	0.3563	20.0055	50.0059	80.0084
Wind power fuzzy + energy storage control curve	0.3552	0.3126	0.4506	20.0167	50.0061	79.9963
Wind power–storage combination fuzzy coefficient control	0.3137	0.3137	0.3126	20.0068	50.0062	80.0084

Figure 15. The simulation results of frequency variation.
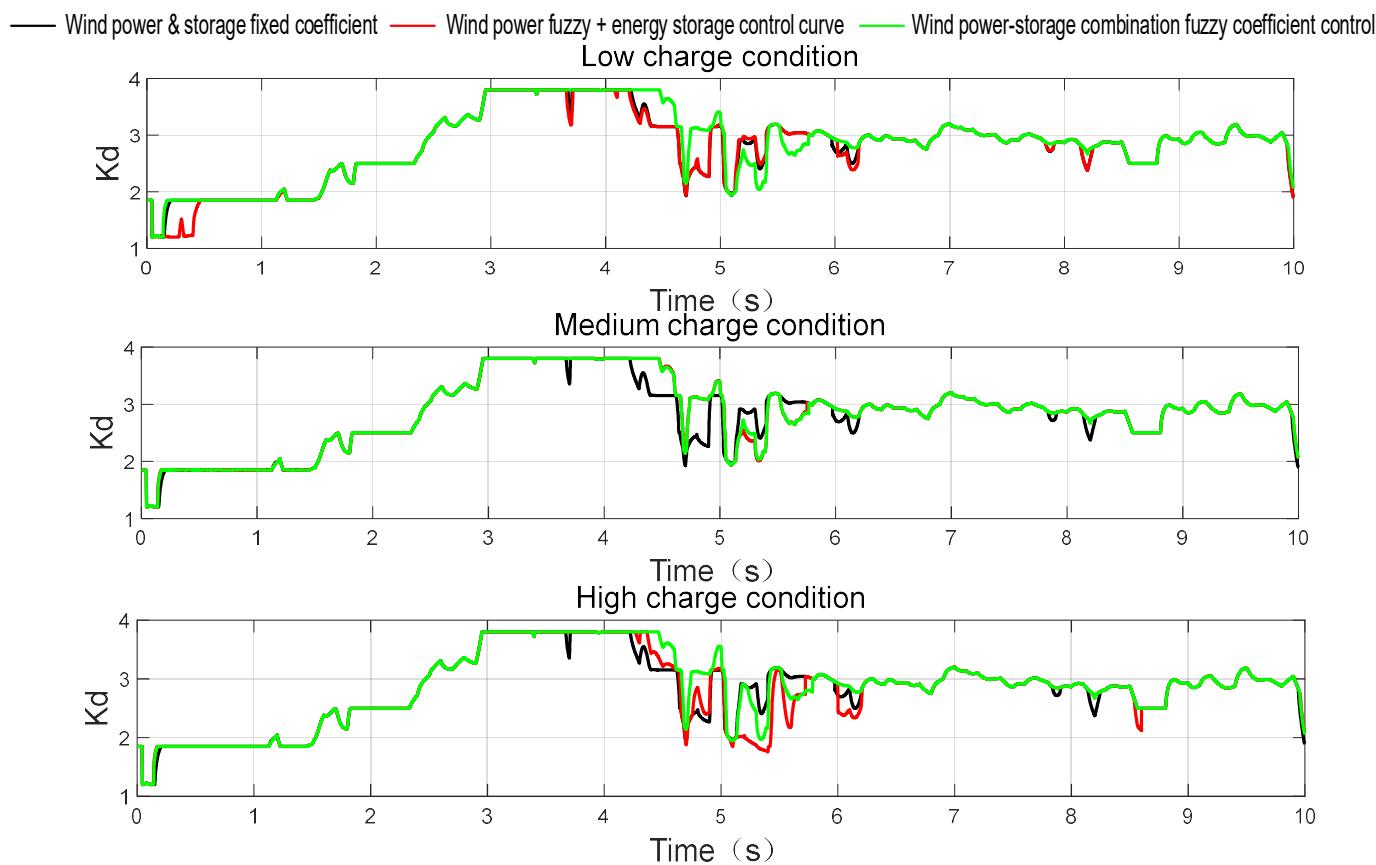
Figure 16. The simulation results of virtual inertia control coefficient.
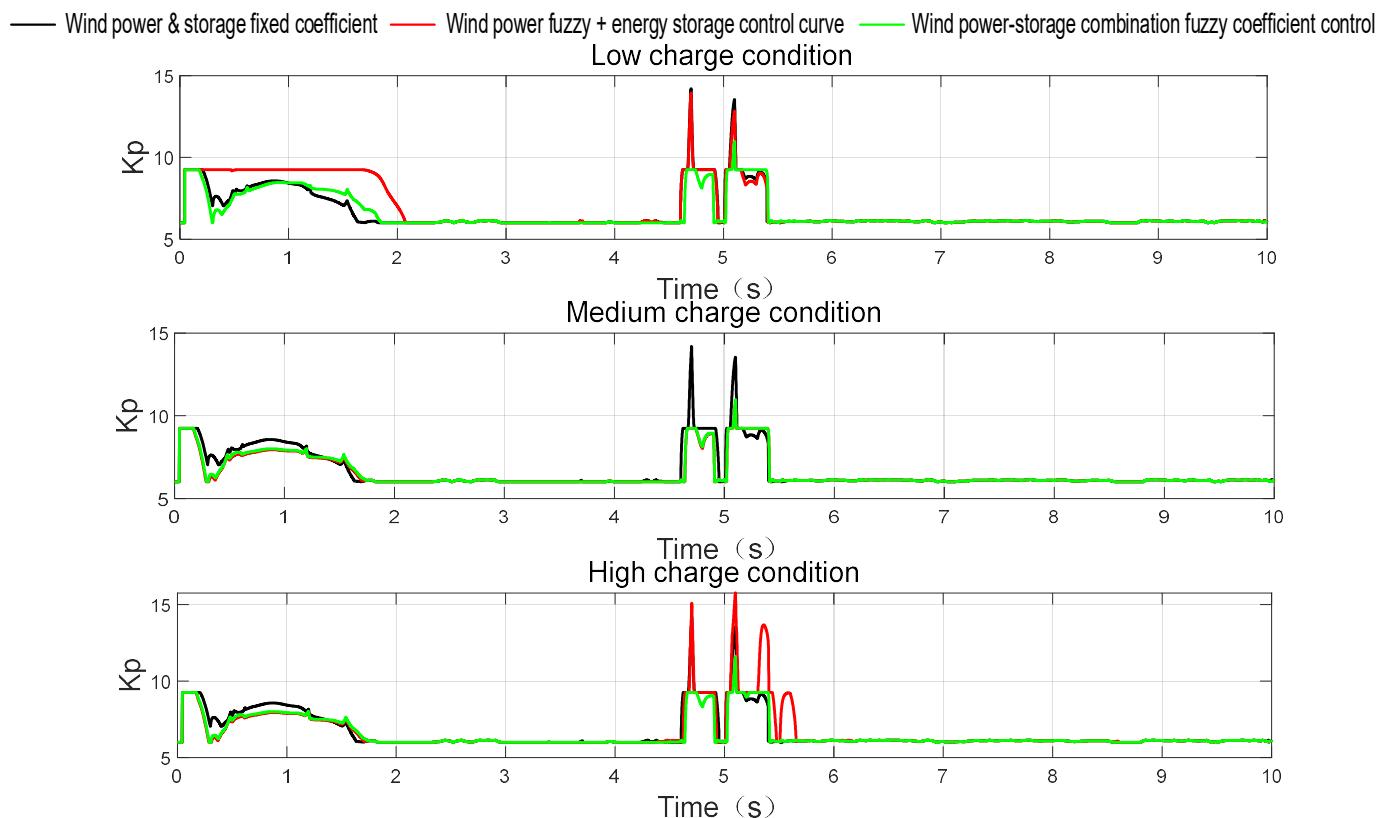
Figure 17. The simulation results of droop control coefficient.
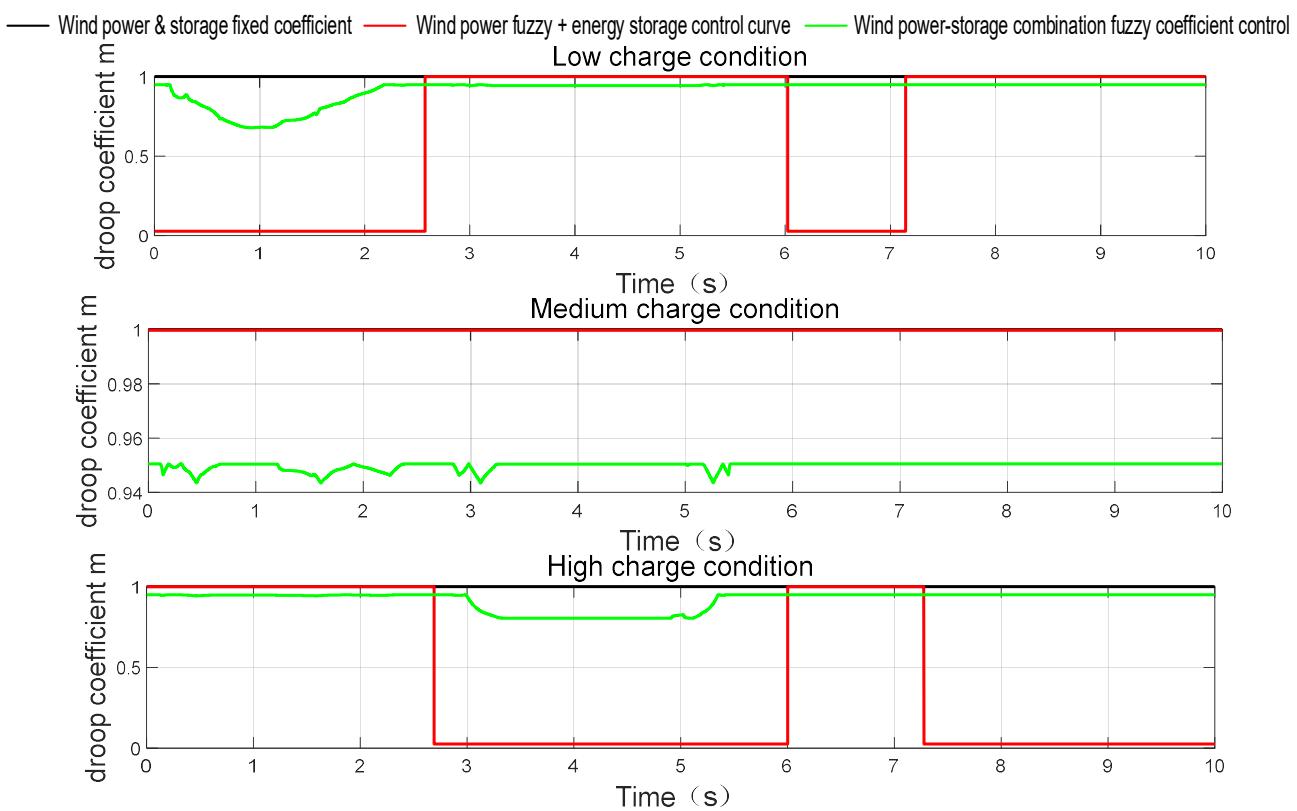
Figure 18. The simulation results of the charge/discharge control factor.
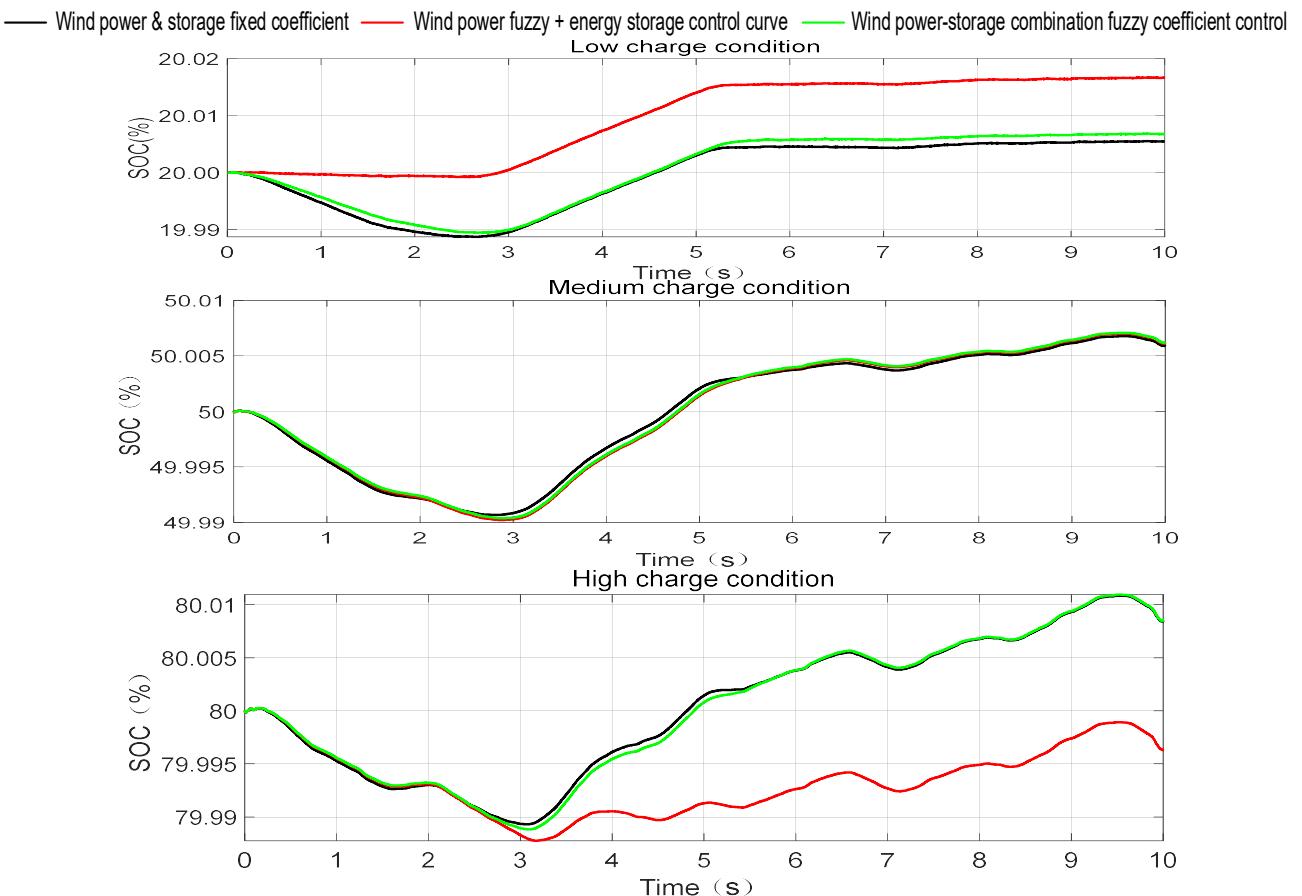
Figure 19. The simulation results of SOC.

4.3. Continuous Working Condition Simulation

To verify the operational capability of the proposed scheme under long-time operating conditions and the robustness of the proposed controller, this paper used a Weber model of wind power generation for simulation with a time duration of 1 h, where the scale parameter was set to 10.53 and the shape parameter was set to 2.315. The simulation results are shown in Figures 20 and 21 and Table 8.

The analysis of the simulation results shows that the proposed control strategy effectively controls the energy storage SOC without affecting the frequency regulation results. The soc is effectively controlled by 2.1 percentage points during one hour of operation. In addition, the results also verify that the proposed control strategy improves the sudden change regulation performance for the continuous regulation of parameters and avoids additional frequency disturbances due to sudden parameter changes.

Table 8. Comparison of results at continuous working condition.

| Parameters	Average Frequency (Hz)		Final SOC (%)	
	Medium-Charge Condition	High-Charge Condition	Medium-Charge Condition	High-Charge Condition
Wind power and storage fixed coefficient	49.9794	49.9794	26.2883	58.3845
Wind power fuzzy + energy storage control curve	49.9792	49.9794	28.9737	57.1203
Wind power–storage combination fuzzy coefficient control	49.9793	49.9793	27.5356	59.2084
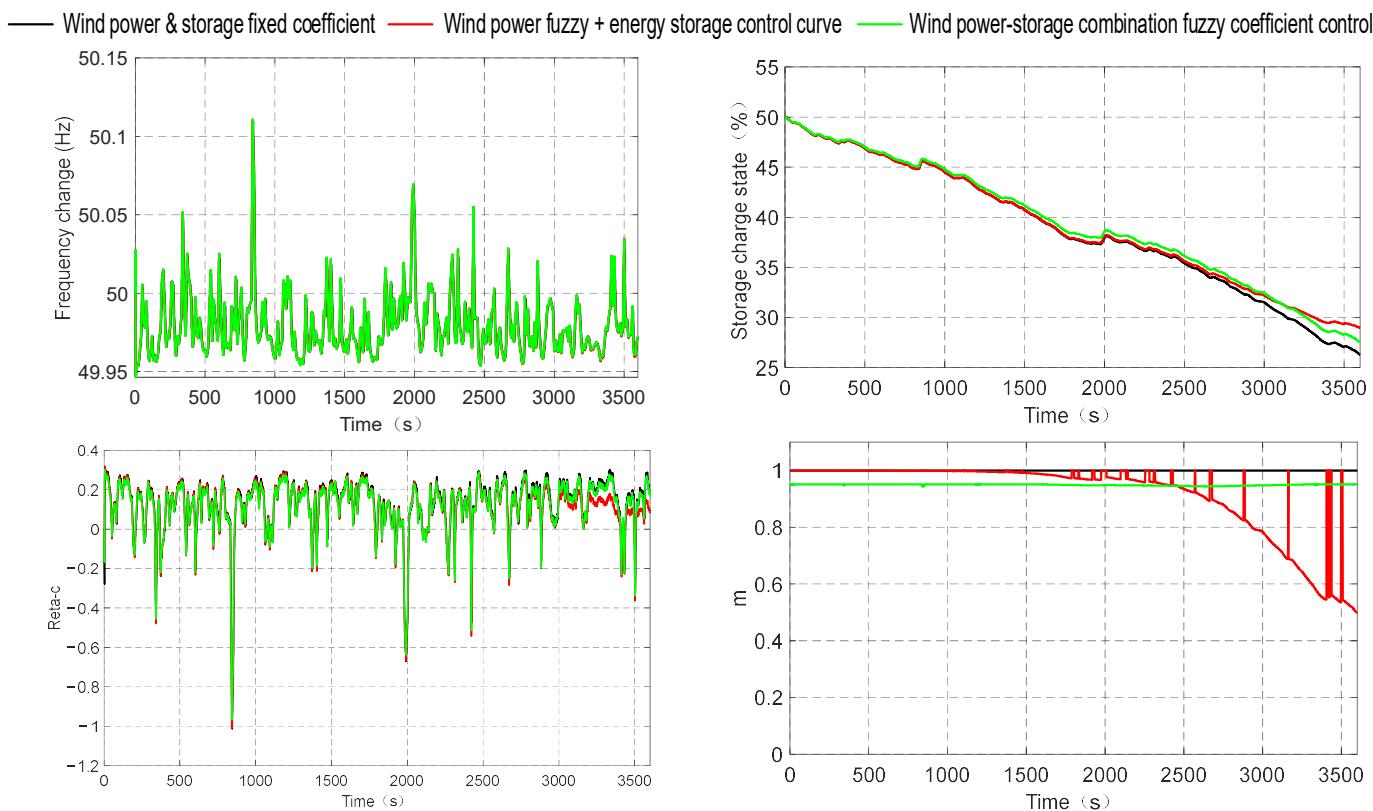
Figure 20. Simulation results of medium-charge state.
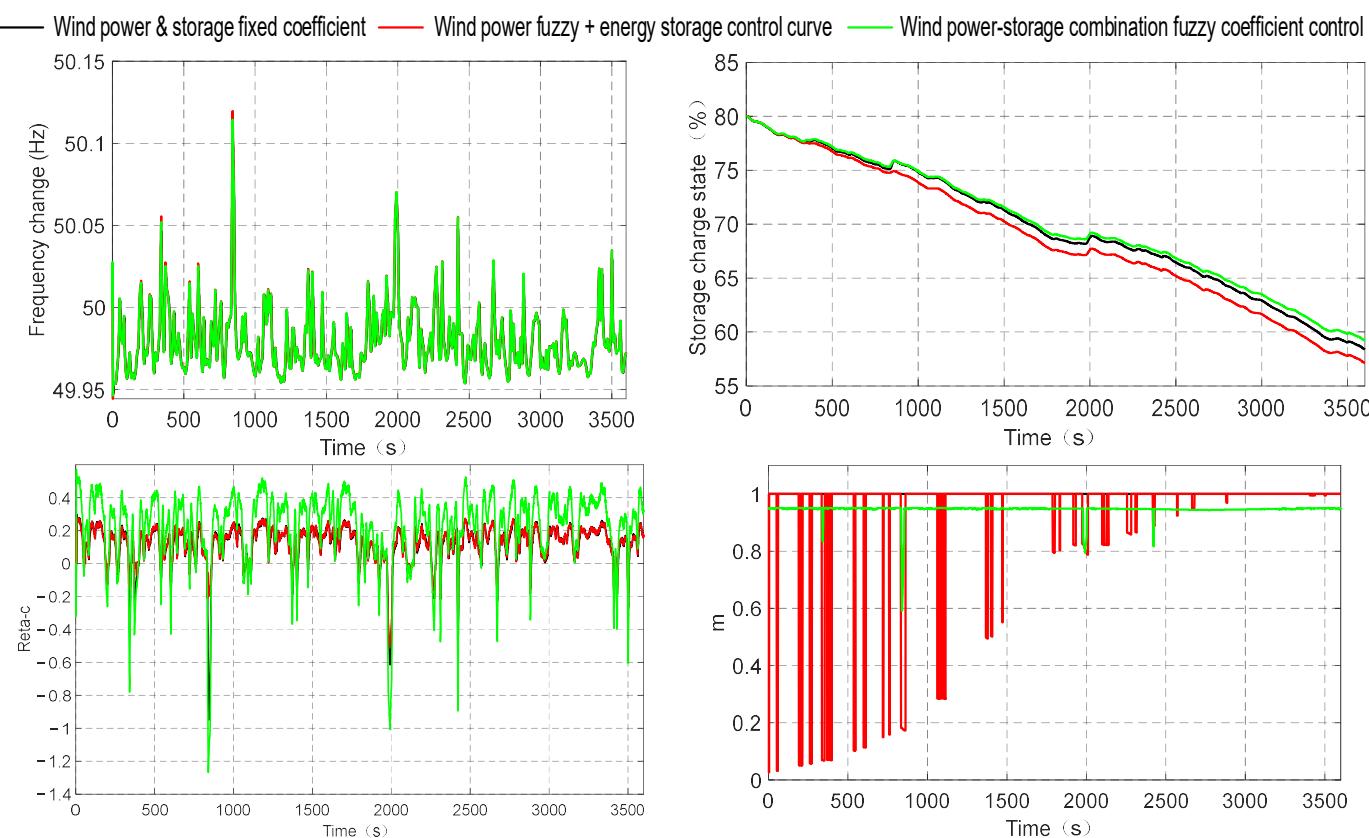
Figure 21. Simulation results of high-charge state.

5. Conclusions

This paper analyzed the frequency regulation performance of the wind storage system and clarified the role of wind power and energy storage in collaborative operation. A novel combination fuzzy controller was established. The controller considered the frequency change in the power system, the wind turbine's operation, and the battery's SOC. The proposed controller achieved an improvement in battery energy utilization efficiency based on the improvement in the frequency regulation performance of the wind storage system. The proposed control achieved good results in the simulation of multiple time scales. In the simulation of step dynamic performance, the proposed controller max improved the tracking effect by no less than 15%. In the simulation of abrupt wind speed, the frequency deviation was reduced by 30.6%. The proposed control strategy can reduce energy consumption by 2.1 percentage points per hour in continuous simulation.

Appendix A

**Figure A1.** Simulation modeling of cases.
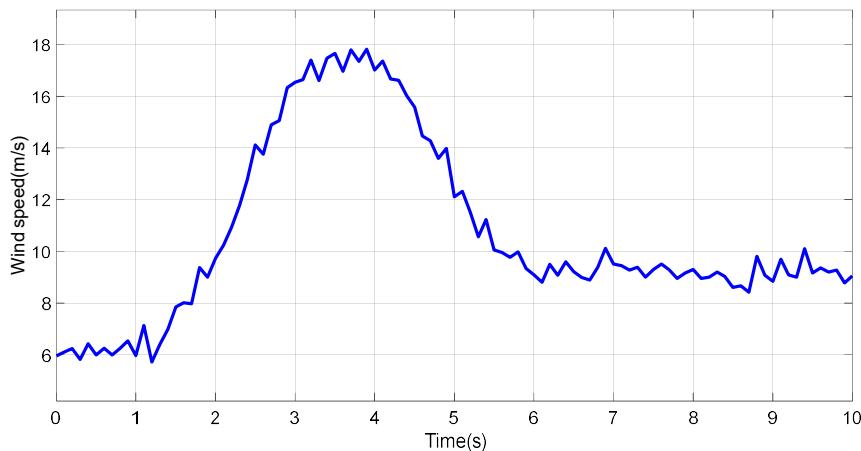
Figure A2. Schematic of wind speed.

References

1. Ding, H.; Pinson, P.; Hu, Z.; Song, Y. Integrated Bidding and Operating Strategies for Wind-Storage Systems. *IEEE Trans. Sustain. Energy* **2016**, *7*, 163–172. [CrossRef]
2. Wei, X.; Xiang, Y.; Li, J.; Zhang, X. Self-Dispatch of Wind-Storage Integrated System: A Deep Reinforcement Learning Approach. *IEEE Trans. Sustain. Energy* **2022**, *13*, 1861–1864. [CrossRef]
3. Dicorato, M.; Forte, G.; Pisani, M.; Trovato, M. Planning and Operating Combined Wind-Storage System in Electricity Market. *IEEE Trans. Sustain. Energy* **2012**, *3*, 209–217. [CrossRef]
4. Yao, J.; Yu, M.; Gao, W.; Zeng, X. Frequency Regulation Control Strategy for PMSG Wind-power Generation System with Flywheel Energy Storage Unit. *IET Renew. Power Gener.* **2017**, *11*, 1082–1093. [CrossRef]
5. Peng, B.; Zhang, F.; Liang, J.; Ding, L.; Liang, Z.; Wu, Q. Coordinated control strategy for the short-term frequency response of a DFIG-ES system based on wind speed zone classification and fuzzy logic control. *Electr. Power Energy Syst.* **2019**, *107*, 363–378. [CrossRef]
6. Zhao, J.; Lyu, X.; Fu, Y.; Hu, X.; Li, F. Coordinated microgrid frequency regulation based on DFIG variable coefficient using virtual inertia and primary frequency control. *IEEE Trans. Energy Convers.* **2016**, *31*, 833–845. [CrossRef]
7. Choi, J.W.; Heo, S.Y.; Kim, M.K. Hybrid Operation Strategy of Wind Energy Storage System for Power Grid Frequency Regulation. *IET Gener. Transm. Distrib.* **2016**, *10*, 736–749. [CrossRef]
8. Zhang, F.; Hu, Z.; Xie, X.; Zhang, J.; Song, Y. Assessment of the Effectiveness of Energy Storage Resources in the Frequency Regulation of a Single-Area Power System. *IEEE Trans. Power Syst.* **2017**, *32*, 3373–3380. [CrossRef]
9. He, G.; Chen, Q.; Kang, C.; Xia, Q.; Poolla, K. Cooperation of Wind Power and Battery Storage to Provide Frequency Regulation in Power Markets. *IEEE Trans. Power Syst.* **2017**, *32*, 3559–3568. [CrossRef]
10. Zang, Y.; Ge, W.; Wang, S.; Zhao, L.; Tan, C. An Economical Optimization Method for Active Power with Variable Droop Control Considering Frequency Regulation Costs in Integrated Energy Systems. *Front. Energy Res.* **2022**, *10*, 905454. [CrossRef]
11. Knap, V.; Chaudhary, S.K.; Stroe, D.-I.; Swierczynski, M.J.; Craciun, B.-I.; Teodorescu, R. Sizing of an Energy Storage System for Grid Inertial Response and Primary Frequency Reserve. *IEEE Trans. Power Syst.* **2016**, *31*, 3447–3456. [CrossRef]
12. Akram, U.; Mithulananthan, N.; Shah, R.; Pourmousavi, S.A. Sizing HESS as Inertial and Primary Frequency Reserve in Low Inertia Power System. *IET Renew. Power Gener.* **2021**, *15*, 99–113. [CrossRef]
13. Yang, L.; Liu, T.; Hill, D.J. Distributed MPC-Based Frequency Control for Multi-Area Power Systems with Energy Storage. *Electr. Power Syst. Res.* **2021**, *190*, 106642. [CrossRef]
14. Yu, B.; Lv, Q.; Zhang, Z.; Dong, H. Hierarchical Distributed Coordinated Control for Battery Energy Storage Systems Participating in Frequency Regulation. *Energies* **2022**, *15*, 7283. [CrossRef]
15. Bai, J.; Zhao, Y.; Jiang, H.; Wei, M.; Yu, S. Load Frequency Control of Power System with Energy Storage Based on Disturbance Observer. *Energy Rep.* **2022**, *8*, 615–622. [CrossRef]
16. Pradhan, C.; Bhende, C.N.; Samanta, A.K. Adaptive Virtual Inertia-Based Frequency Regulation in Wind Power Systems. *Renew. Energy* **2018**, *115*, 558–574. [CrossRef]
17. Guan, M. Scheduled Power Control and Autonomous Energy Control of Grid-Connected Energy Storage System (ESS) With Virtual Synchronous Generator and Primary Frequency Regulation Capabilities. *IEEE Trans. Power Syst.* **2022**, *37*, 942–954. [CrossRef]
18. Ge, S.; He, X.; Liu, H.; Mi, Y.; Wang, C. Frequency Coordinated Control Strategy Based on Sliding Mode Method for a Microgrid with Hybrid Energy Storage System. *IET Gener. Transm. Distrib.* **2021**, *15*, 1962–1971. [CrossRef]
19. Li, P.; Tan, Z.; Zhou, Y.; Li, C.; Li, R.; Qi, X. Secondary Frequency Regulation Strategy with Fuzzy Logic Method and Self-Adaptive Modification of State of Charge. *IEEE Access* **2018**, *6*, 43575–43585. [CrossRef]

20. Yu, Y.; Qin, Y.; Gong, H. Fuzzy Q-Learning Algorithm for Storage Optimization in Islanding Microgrid. *J. Electr. Eng. Technol.* **2021**, *16*, 2343–2353. [CrossRef]

21. Yin, L.; Li, Y. Fuzzy Vector Reinforcement Learning Algorithm for Generation Control of Power Systems Considering Flywheel Energy Storage. *Appl. Soft Comput.* **2022**, *125*, 109149. [CrossRef]

22. Zertek, A.; Verbic, G.; Pantos, M. A novel strategy for variable-speed wind turbines' participation in primary frequency control. *IEEE Trans. Sustain. Energy* **2012**, *3*, 791–799. [CrossRef]

23. Wang, Y.; Delille, G.; Bayem, H.; Guillaud, X. High wind power penetration in isolated power systems: Assessment of wind inertial and primary frequency responses. *IEEE Trans. Power Syst.* **2013**, *28*, 2412–2420. [CrossRef]

24. Kroposki, B.; Johnson, B.; Zhang, Y.; Gevorgian, V.; Denholm, P.; Hodge, B.M.; Hannegan, B. Achieving a 100% renewable grid: Operating electric power systems with extremely high levels of variable renewable energy. *IEEE Power Energy Mag.* **2017**, *15*, 61–73. [CrossRef]

25. Lalor, G.; Mullane, A.; O'Malley, M. Frequency control and wind turbine technologies. *IEEE Trans. Power Syst.* **2005**, *20*, 1905–19135. [CrossRef]

26. Ochoa, D.; Martinez, S. Fast-frequency response provided by DFIG-wind turbines and its impact on the grid. *IEEE Trans. Power Syst.* **2017**, *32*, 4002–4011. [CrossRef]

27. Fu, Y.; Wang, Y.; Zhang, X. Integrated wind turbine controller with virtual inertia and primary frequency responses for grid dynamic frequency support. *IET Renew. Power Gener.* **2017**, *11*, 1129–1137. [CrossRef]

28. Dubarry, M.; Truchot, C.; Liaw, B.Y. Cell degradation in commercial LiFePO4 cells with high-power and high-energy designs. *J. Power Sources* **2014**, *258*, 408–419. [CrossRef]

29. Dubarry, M.; Liaw, B.Y.; Chen, M.-S.; Chyan, S.-S.; Han, K.-C.; Sie, W.-T.; Wu, S.-H. Identifying batteryaging mechanisms in large format Liion cells. *J. Power Sources* **2011**, *196*, 3420–3425. [CrossRef]